NACA

RESEARCH MEMORANDUM

INVESTIGATION AT SUPERSONIC SPEEDS OF A TRANSLATING -

SPIKE INLET EMPLOYING A STEEP-LIP COWL

By Gerald C. Gorton

Lewis Flight Propulsion Laboratory Cleveland, Ohio

NATIONAL ADVISORY COMMITTEE FOR AERONAUTICS

WASHINGTON

October 11, 1954
Declassified October 16, 1961

NATIONAL ADVISORY COMMITTEE FOR AERONAUTICS

RESEARCH MEMORANDUM

INVESTIGATION AT SUPERSONIC SPEEDS OF A TRANSLATING-SPIKE

INLET EMPLOYING A STEEP-LIP COWL

By Gerald C. Gorton

SUMMARY

An experimental investigation was conducted in the Lewis 8- by 6foot supersonic wind tunnel at stream Mach numbers of 1.5, 1.8, and 2.0 on a translating-spike inlet analytically designed to keep the cone shoulder downstream of the cowl-lip station without a net internal contraction.

The present inlet, which incorporates an internal cowl-lip angle of 17.5° , was constructed to have the same inlet capture area and maximum cross-sectional area as that of a previously investigated translating-spike inlet which had an internal cowl-lip angle of only 7° .

The pressure recovery at critical operation was increased significantly over the inlet with a low cowl-lip angle, except for the extreme forward spike positions at stream Mach numbers of 1.8 and 2.0. This gain in pressure recovery was at the expense of a higher cowl pressure drag and a decreased stable mass-flow range.

At critical operation the increased pressure recovery more than compensated for the higher cowl pressure drag, and resulted in a significant gain in effective thrust.

INTRODUCTION

Analysis and experimental evaluation of translating-spike inlets indicate that such inlets can satisfy the jet-engine air flow requirements while operating near the optimum inlet condition. The design of translating-spike inlets is complicated, however, by the fact that an inlet designed with a low cowl-lip angle generally experiences internal contraction when the spike is retracted. As shown in references 1 and 2, excessive internal contraction results in lower pressure recovery and higher drag at critical flow. With the spike extended a loss in pressure recovery may again result if at critical flow the cone shoulder is located in a supersonic-flow region.

In a discussion of the design problems associated with translating-spike inlets, it was stated (ref. 1) that an inlet could be designed to keep the cone shoulder downstream of the cowl lip for the entire range of spike translation without internal contraction. An analytical expression has been derived describing such an inlet (see appendix) and an 8-inch-diameter model based on this design criterion was constructed and evaluated in the NACA Lewis 8- by 6-foot supersonic wind tunnel. The results of this investigation are presented herein.

SYMBOLS

The following symbols are used throughout the report:

A flow area, sq ft

A_m maximum external cross-sectional area, 0.360 sq ft

C_D external-drag coefficient, D/q_OA_m

 $C_{_{\overline{U}},\overline{D}}$ coefficient of thrust minus drag

D drag force, lb

F thrust with actual total-pressure recovery, lb

F, thrust with 100 percent total-pressure recovery, lb

M Mach number

m mass flow, slugs/sec

mass flow through stream tube defined by cowl-lip area, slugs/sec

P total pressure, lb/sq ft

p static pressure, lb/sq ft

q dynamic pressure, $\gamma pM^2/2$, lb/sq ft

 $\frac{W\sqrt{\theta}}{8A}$ corrected air-flow parameter, lb/(sec)(sq ft)

W air flow, lb/sec

x axial distance downstream of cowl lip, in.

- α angle of attack, deg
- γ ratio of specific heats for air, 1.4 for calculations reported herein
- δ total pressure divided by NACA standard sea-level static pressure
- θ stream total temperatures divided by NACA standard sea-level static temperature
- cowl-position parameter (angle between axis of diffuser and line joining apex of cone to cowl lip), deg

Subscripts:

- O free stream
- 3 plane of survey

APPARATUS AND PROCEDURE

The 8-inch diameter translating-spike-inlet model was sting-mounted in the 8- by 6-foot supersonic wind tunnel and investigated at Mach numbers Mo of 1.5, 1.8, and 2.0. The Reynolds number was approximately 3.4×10⁶ based on the maximum external diameter of the model (8.125 in.).

The basic model (see fig. 1) was identical to the model of reference l with the exception of the inlet cowl and the conical-spike centerbody. The inlet cowl and the conical-spike centerbody (see table I for coordinates) were designed to have the cone shoulder at the cowl-lip station for the most forward spike position ($\theta_{\ell} = 34^{\circ}$) and to allow retraction of the spike to $\theta_{\ell} = 54^{\circ}$ without a net internal contraction (see fig. 2 for diffuser-flow-area variation). The analytical design procedure is shown in the appendix.

In order to achieve such a design, it was necessary, as shown in the appendix, to utilize an internal cowl-lip angle of 17.5° compared with the 7° internal cowl-lip angle of the model of reference 1. However, to facilitate comparison between the two models, the same inlet diameter of 5.32 inches was maintained. It was necessary, however, to increase length of the present model by 1.34 inches. In addition, cylindrical spacers were used to simulate spike translation rather than faired spacers as were used in the model of reference 1. Cylindrical spacers more nearly represent the translating mechanism that would be used in a practical inlet.

The instrumentation consisted of a static-pressure rake at station 3, a three-component strain-gage balance within the model centerbody, a movable plug at the exit of the model with which to vary the mass flow, a direct-reading angle-of-attack indicator, and a dynamic pressure pickup located slightly downstream from the plane of survey. The dynamic pressure pickup was used in conjunction with schlieren apparatus to evaluate inlet-flow instability. The onset of instability was abrupt enough to allow reasonable accuracy in determining the mass-flow ratio at which pulsing started.

The mass-flow ratio presented is the ratio of mass flow through the model m_3 to that mass flow m_0 of a free-stream tube defined by the capture area of the inlet cowl. The mass flow was calculated by assuming a choked condition at the exit-nozzle throat and using the measured average static pressure and the calculated diffuser Mach number at the plane of survey. The Mach number at the plane of survey was determined from the area ratio existing between the plane of survey and the choked exit assuming isentropic one-dimensional flow. This Mach number was converted

to a corrected air-flow parameter $\frac{W_3\sqrt{\theta_3}}{\delta_3A_3}$ for convenient application to engine-inlet matching.

Total-pressure recovery is the ratio of the total pressure P_3 , determined from the measured average static pressure and the calculated Mach number at the plane of survey, to the measured free-stream total pressure P_0 .

External-drag and thrust-minus-drag coefficients were computed from axial-force readings of the strain-gage balance in conjunction with internal-pressure measurements. The forces on the mass-flow plug were not registered by the strain-gage balance.

The effective thrust parameter $\frac{F-D}{F_1}$ was calculated according to the method set forth in reference 3, using the measured inlet pressure recovery and the drag data in conjunction with known engine specifications and air-flow requirements.

DISCUSSION OF RESULTS

Total-pressure recovery P_3/P_0 for the range of cowl-position parameter investigated is presented in figures 3(a) to (f) for stream Mach numbers M_0 of 1.5, 1.8, and 2.0 for angles of attack of 0° , 3° , 6° , and 9° . The external drag coefficients and corrected air-flow parameter for zero angle of attack are also included. These performance characteristics are presented as a function of mass-flow ratio m_3/m_0 .

Figure 4 shows the variation in stable mass-flow range as a function of spike translations for various angles of attack. The inlet of the present investigation has less stable mass-flow range than the translating-spike inlet reported in reference 1. It should be noted that aside from the difference in internal cowl-lip angles there was considerable difference in the diffuser-area variations of the two models. The model of reference 1 had an essentially constant area section for the initial portion of the diffuser, while the present model initially diffused quite rapidly at most of the spike positions. A constant-area section has been shown to be an effective way to increase the stable mass-flow range of an annular inlet (see ref. 4).

The effect of spike translation on the inlet performance at critical operation is presented in figure 5 for zero angle of attack. Pressure recovery is generally raised as the spike is translated to values of cowl-position parameter θ_{ℓ} less than 54. This increase is mainly the result of increasing the amount of flow passing an oblique shock prior to the normal shock. However, the pressure recovery does start to decrease quite abruptly at the extreme forward spike positions. This may indicate that the rate of diffusion is too rapid, causing separation losses. Concurrently the normal shock is in the vicinity of the cone shoulder and possibly may result in reexpansion losses.

The external drag coefficients presented in figure 5 indicate the variation of critical flow drag with spike translation. It should be noted that at $M_{\rm O}=2.0$ the fairing of the drag curve between $\theta_{\rm Z}=45.6^{\rm O}$ and $42.8^{\rm O}$ is arbitrary, since the exact $\theta_{\rm Z}$ at which the drag increased was not established. A few typical schlieren photographs are shown in figure 6 for various values of spike position. Note that at $M_{\rm O}=1.5$, the cowl-lip angle was steep enough to cause a detached shock to form at the cowl lip.

Angle-of-attack performance at critical operation is shown in figure 7. Pressure recovery appears to be generally more sensitive to angle of attack when the spike is in the forward positions.

The comparisons of the present translating-spike inlet and the translating-spike inlet of reference 1 are shown in figures 8 to 10. Figure 8 compares the zero-angle-of-attack critical-flow pressure recovery and drag performance as a function of spike translation. At a stream Mach number of 2.0 with the oblique shock at the cowl lip, there was a gain in recovery of $3\frac{1}{2}$ percent of free-stream total pressure over the inlet of reference 1. With the spike positioned for approximately 10 percent oblique shock spillage ($\theta_{1} = 39$) the gain was about 5 percent and was a maximum value. As the spike was translated to values of $\theta_{1} < 39^{\circ}$, the pressure recovery commenced to decrease quite rapidly until at

 θ_l = 35.8 the present inlet started to give poorer pressure-recovery performance than the inlet of reference 1. The same trends occur at M_0 = 1.8. At M_0 = 1.5 the present inlet exhibited superior pressure-recovery performance for the entire range of translation.

The external-drag-coefficient data of figures 8(a) to (c) illustrate the penalty paid, in cowl pressure drag, for the increased pressure recovery. The change in external drag coefficient (0.10 to 0.13) at $\theta_{1}=43^{\circ}$ for $M_{0}=2.0$ indicates the increase in cowl pressure drag resulting from the steep cowl-lip angle, inasmuch as a full stream tube is being captured and the change in friction drag is negligible. However, when the spike was retracted to $\theta_{1}>50^{\circ}$ at $M_{0}=1.5$ the external drag coefficient was lower than that of the translating-spike inlet of reference 1. This results from the fact that the present inlet spills less mass flow than the inlet of reference 1. The spillage with the present inlet results from the detached shock at the cowl lip, whereas the inlet of reference 1 experienced spillage because of excessive internal contraction.

Since the over-all evaluation depends on the combination of drag and pressure recovery, thrust-minus-drag coefficients calculated from model-balance measurements are presented for critical operation in figure 9. The present inlet shows increased thrust-minus-drag performance over the translating-spike inlet of reference 1 except for the extreme forward spike positions at $M_{\odot}=1.8$ and 2.0 where the pressure-recovery performance decreased quite rapidly.

A more practical evaluation of the superiority of the present translating-spike inlet over the one of reference 1 is shown in figure 10 where a typical turbojet engine is matched to both inlets over the Mach number range from 1.5 to 2.0. Both inlets were sized for zero spillage at $M_{\rm O}=2.0$. At the lower Mach numbers, matching at critical operation was accomplished by translating the spike.

The effective thrust parameter $\frac{F-D}{F_1}$ is increased 6 percent at $M_0=2.0$, 6 percent at $M_0=1.8$, and 14 percent at $M_0=1.5$ by using the translating-spike inlet of the present investigation. The increased gain at $M_0=1.5$ results from the elimination of internal contraction. The excessive internal contraction present with the inlet of reference 1 caused more spillage than the amount required for matching at critical operation, thus requiring the inlet to operate supercritically. The present translating-spike inlet allowed matching at critical operation.

The comparison presented based on an inlet sized for zero spillage at $M_{\rm O}=2.0$ does not allow the present inlet to take advantage of the increase in pressure recovery available by sizing for some oblique shock spillage at $M_{\rm O}=2.0$. On this basis, the present inlet is capable of showing even greater advantage over the inlet of reference 1.

SUMMARY OF RESULTS

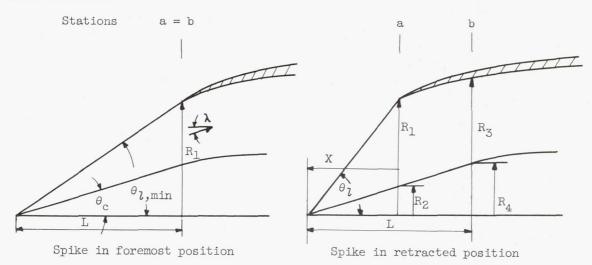
The following results were obtained from an analytical and experimental investigation at Mach numbers 1.5, 1.8, and 2.0 of a translating-spike inlet:

- 1. A translating-spike inlet can be designed, from an analytical expression, which will keep the cone shoulder downstream of the cowl lip without the necessity of internal contraction.
- 2. The pressure recovery at critical operation increased significantly over an inlet having a low cowl-lip angle except for the extreme forward positions of the spike at $M_0 = 1.8$ and 2.0. This gain in pressure recovery was at the expense of higher cowl pressure drags and a decreased stable mass-flow range.
- 3. The increased pressure recovery more than compensated for the higher cowl pressure drag, and resulted in a significant gain in effective thrust.

Lewis Flight Propulsion Laboratory
National Advisory Committee for Aeronautics
Cleveland, Ohio, August 3, 1954

APPENDIX - DERIVATION OF EQUATIONS DESCRIBING COWL-LIP SHAPE

The internal cowl-lip shape of a translating-spike inlet, which will allow translation of the cone shoulder downstream of the cowl lip (see following sketches) without a net internal contraction, can be described by an analytical expression. The derivation of this expression is presented herein.



- a cowl-lip station
- b cone-shoulder station
- L length of conical portion of spike, in.
- R radius normal to model axis
- X spike tip projection, in.
- θ cone half-angle, deg
- $\theta_{l, \min}$ cowl-position parameter for most forward position of spike (cone shoulder at cowl-lip station), deg
- λ_{a} average flow angle at station a
- λ_{b} average flow angle at station b

The derivation of the following analytical expressions is based on the condition that the flow area at station a be equal to the flow area at station b when the spike is fully retracted (X = 0).

G

Flow area at station
$$a = \pi(R_1^2 - R_2^2) \cos \lambda_a$$
 (1)

Flow area at station
$$b = \pi(R_3^2 - R_4^2) \cos \lambda_b$$
 (2)

Therefore:

$$\pi(R_1^2 - R_2^2) \cos \lambda_a = \pi(R_3^2 - R_4^2) \cos \lambda_b$$
 (3)

From the preceding sketches,

$$R_1 = L \tan \theta_{l,min}$$
 (Spike in foremost position) (4)

$$R_2 = X \tan \theta_c$$
 (5)

$$R_4 = L \tan \theta_c$$
 (6)

Thus substitution of equations (4) to (6) into equation (3) results in the following expression for the internal radius of the cowl at the coneshoulder station, for a given spike position:

$$\left[\left(\text{L } \tan \theta_{1,\text{min}}\right)^{2} - \left(\text{X } \tan \theta_{c}\right)^{2}\right] \cos \lambda_{a} = \left[R_{3}^{2} - \left(\text{L } \tan \theta_{c}\right)^{2}\right] \cos \lambda_{b}$$

$$R_3 = \sqrt{\left[\left(L \tan \theta_{1,\min}\right)^2 - \left(X \tan \theta_{c}\right)^2\right] \frac{\cos \lambda_a}{\cos \lambda_b} + \left(L \tan \theta_{c}\right)^2}$$
 (7)

Differentiation of equation (7) with respect to X results in an expression describing the slope of the cowl internal contour. Since the flow angle λ_a is always equal to or greater than λ_b the assumption that $\lambda_a = \lambda_b$ will not influence the equation such as to cause internal contraction; this assumption is made for simplicity and the following equation results:

$$\frac{d(R_3)}{d(x)} = -\frac{x \tan^2 \theta_c}{R_3} \tag{8}$$

For the limit of this equation where X = L,

$$R_3 = R_1 = L \tan \theta_{l,min}$$
 (9)

Substitution of equation (9) in equation (8) will give an expression for the initial internal slope of the cowl lip, as follows:

$$\frac{d(R_3)}{d(X)_{\text{lip}}} = -\frac{\tan^2 \theta_c}{\tan \theta_{l,\text{min}}}$$
 (10)

From equation (10) it is apparent that the internal cowl-lip angle necessary for such an inlet as described herein is a function of the cone half-angle $\theta_{\rm c}$ and the most forward position of the spike, $\theta_{\rm l,min}$, which places the cone shoulder at the cowl-lip station. Figure 11 presents the required initial internal cowl-lip angle for cone half-angles of 20°, 25°, and 30° for a range of minimum cowl-position parameter.

The analytical expression is likewise valid for a multishock inlet where $\theta_{\rm c}$ and $\theta_{\it l,min}$ are determined from the last conical portion of the spike.

The procedure to be followed in a typical design is as follows:

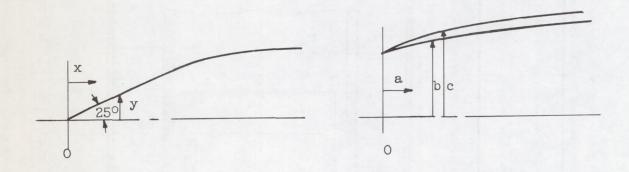
- (1) Affix the inlet capture area and the cone half-angle $\theta_{\rm c}$.
- (2) For the desired forward translation $\theta_{l,min}$ determine the length of the conical portion of the spike, L.
- (3) From equation (10), knowing $\theta_{\rm c}$ and $\theta_{\rm l,min}$, the initial internal cowl-lip angle can be determined.
- (4) From equation (7) (assuming $\lambda_a = \lambda_b$), the coordinates of the cowl can be determined for the desired amount of spike retraction.
- (5) The coordinate of the cowl and centerbody downstream of the cone-shoulder station can now be determined according to the desired maximum model cross-section area and diffuser flow-area variation. It should be noted that the cone shoulder need not be the maximum diameter of centerbody.

REFERENCES

- 1. Gorton, Gerald C.: Investigation of Translating-Spike Supersonic Inlet as Means of Mass-Flow Control at Mach Numbers of 1.5, 1.8, and 2.0. NACA RM E53GlO, 1953.
- 2. Leissler, L. Abbott, and Sterbentz, William H.: Investigation of a Translating-Cone Inlet at Mach Numbers from 1.5 to 2.0. NACA RM E54B23, 1954.
- 3. Kremzier, Emil J.: A Method for Evaluating the Effects of Drag and Inlet Pressure Recovery on Propulsion-System Performance. NACA TN 3261, 1954.
- 4. Nettles, J. C.: The Effect of Initial Rate of Subsonic Diffusion on the Stable Subcritical Mass-Flow Range of a Conical Shock Diffuser. NACA RM E53E26, 1953.

TABLE I. - COORDINATES FOR COWL AND CONICAL SPIKE CENTERBODY

[All dimensions in inches.]



Conical-spike centerbody		Cowl		
х	У	а	ъ	С
0	0	0	2.660	2.660
3.967	Conical	.250	2.734	2.759
4.064	1.886	.500	2.800	2.851
4.214	1.926	1.00	2.918	3.011
4.464	1.976	2.0	3.108	3.215
4.964	2.046	3.0	3.222	3.333
5.964	2.147	4.0	3.277	3.398
6.964	2.191	5.0	3.309	3.434
7.964	2.223	6.0	3.327	3.452
8.964	2.237	7.0	3.334	3.459
9.992	2.250	8.0	3.339	3.464
		9.0	3.350	3.475
	* 1	10.0	3.374	3.499

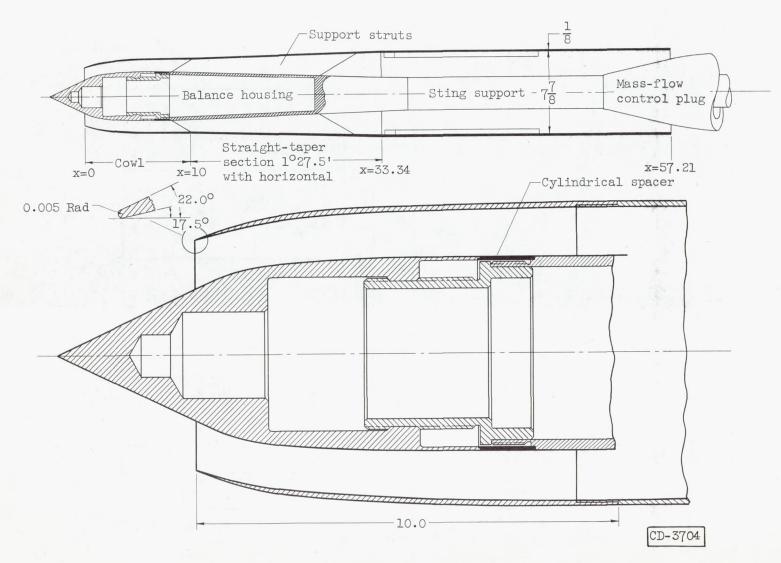


Figure 1. - Schematic diagram of translating-spike inlet model. (All dimensions in inches.)

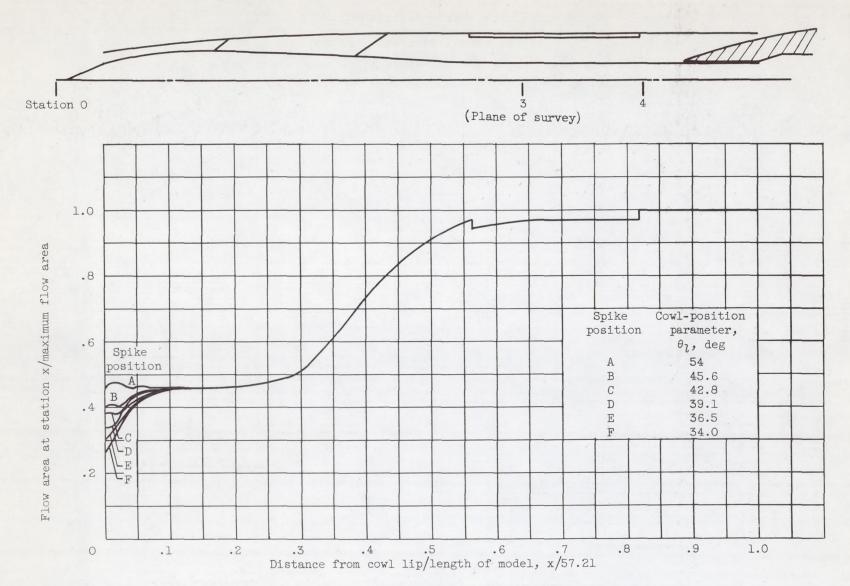


Figure 2. - Diffuser flow-area variation.

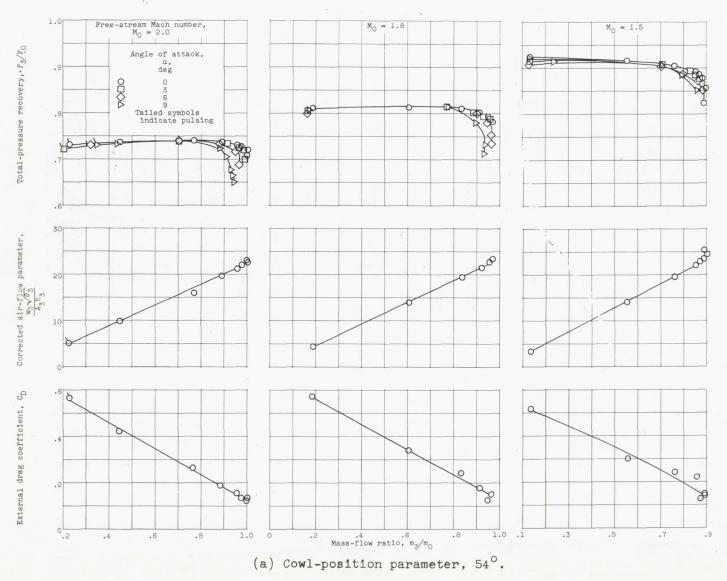


Figure 3. - Translating-spike inlet performance.

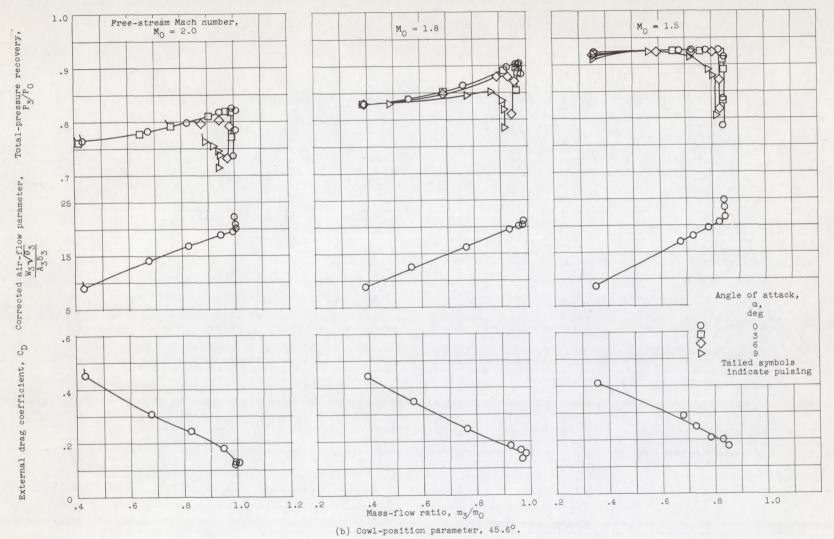


Figure 3. - Continued. Translating-spike inlet performance.

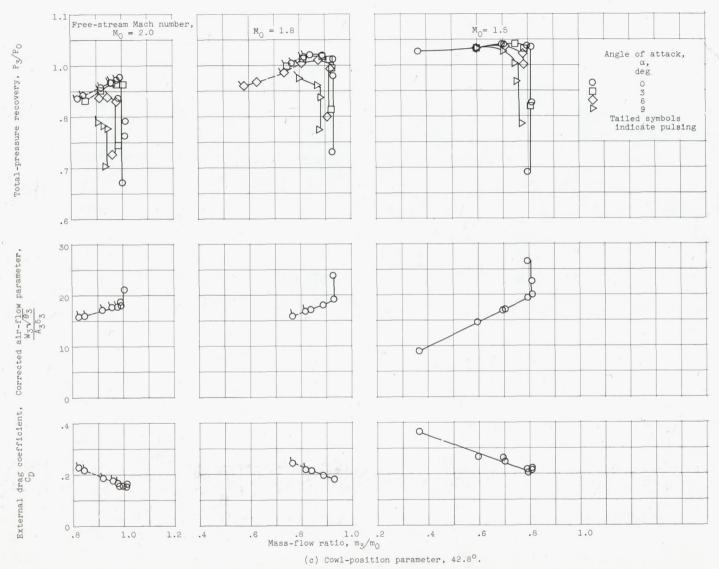


Figure 3. - Continued. Translating-spike inlet performance.

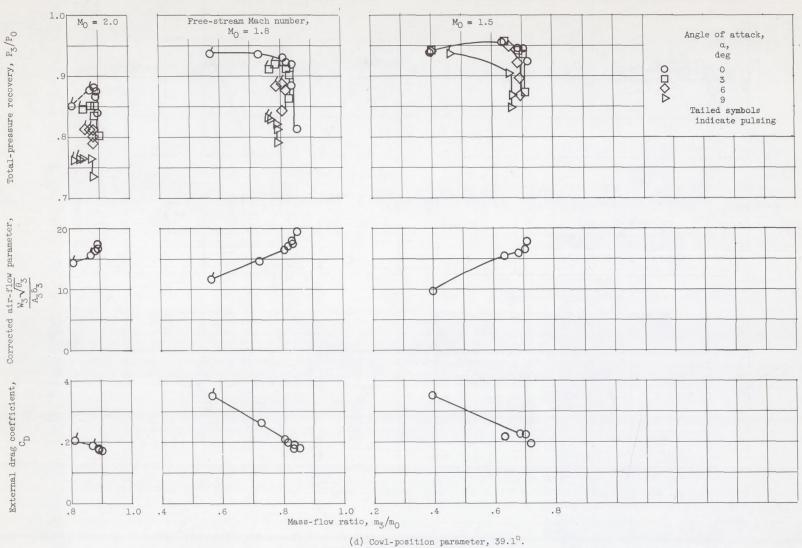


Figure 3. - Continued. Translating-spike inlet performance.

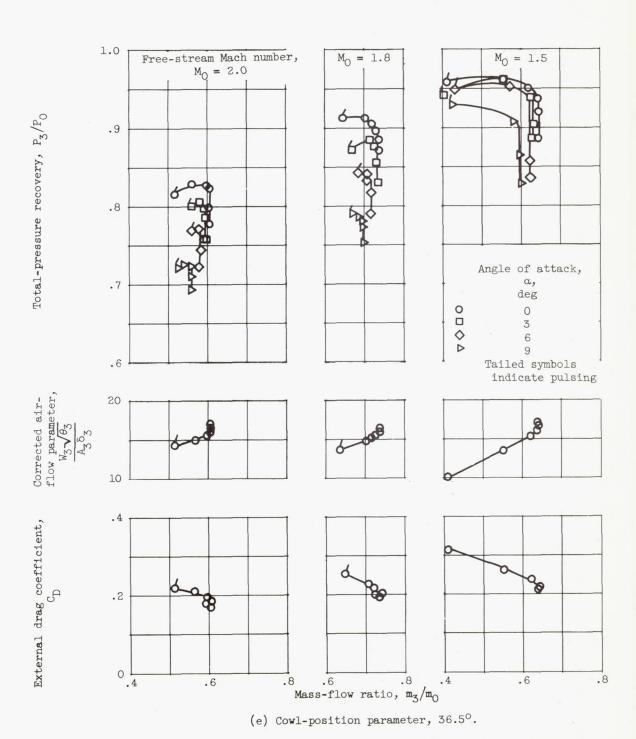


Figure 3. - Continued. Translating-spike inlet performance.

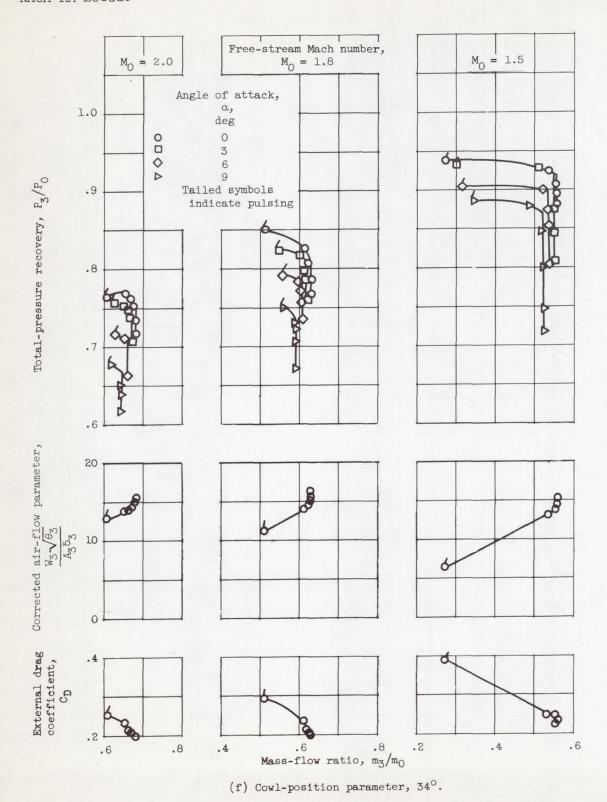


Figure 3. - Concluded. Translating-spike inlet performance.

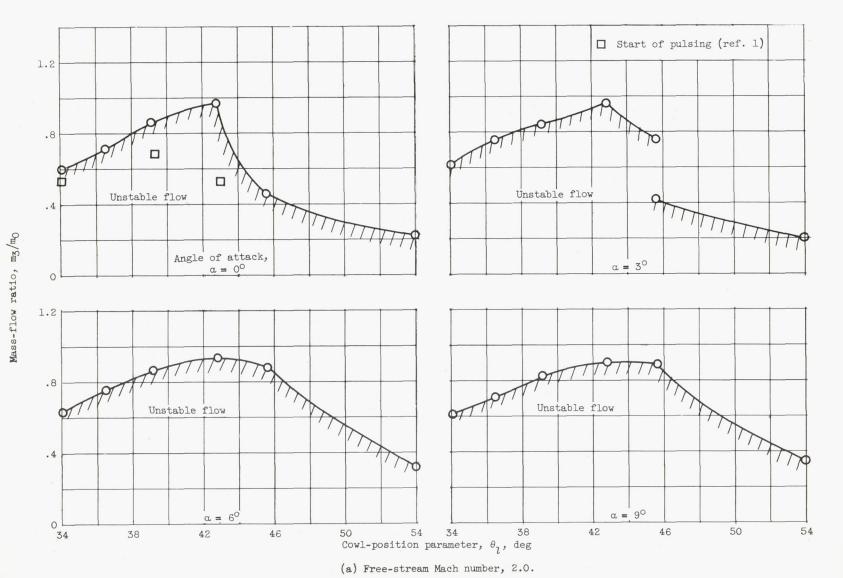


Figure 4. - Stability range of translating-spike inlet.

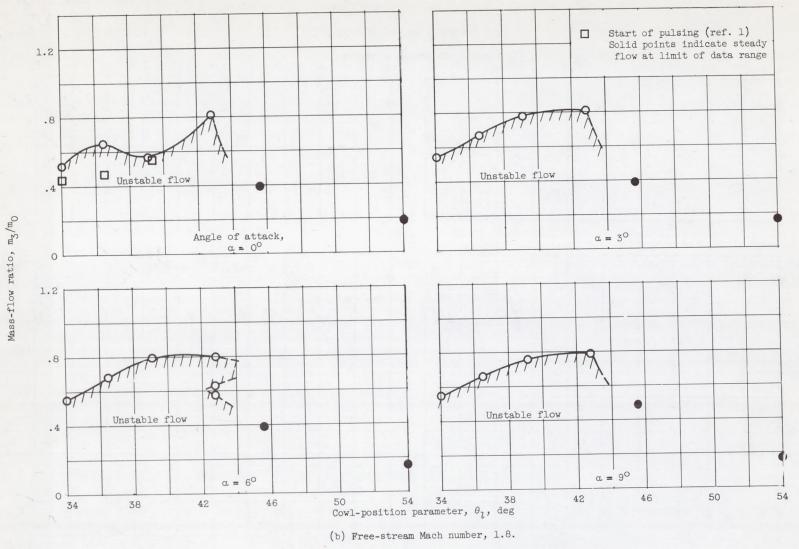


Figure 4. - Continued. Stability range of translating-spike inlet.

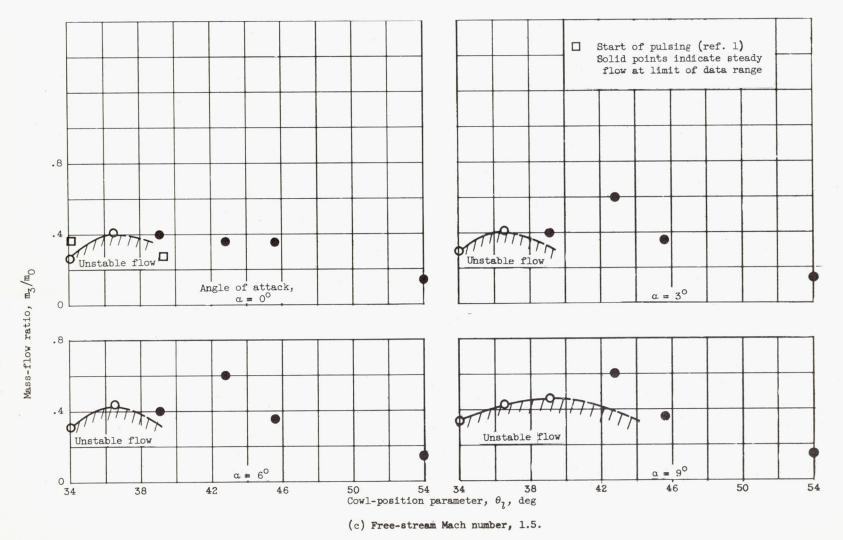


Figure 4. - Concluded. Stability range of translating-spike inlet.

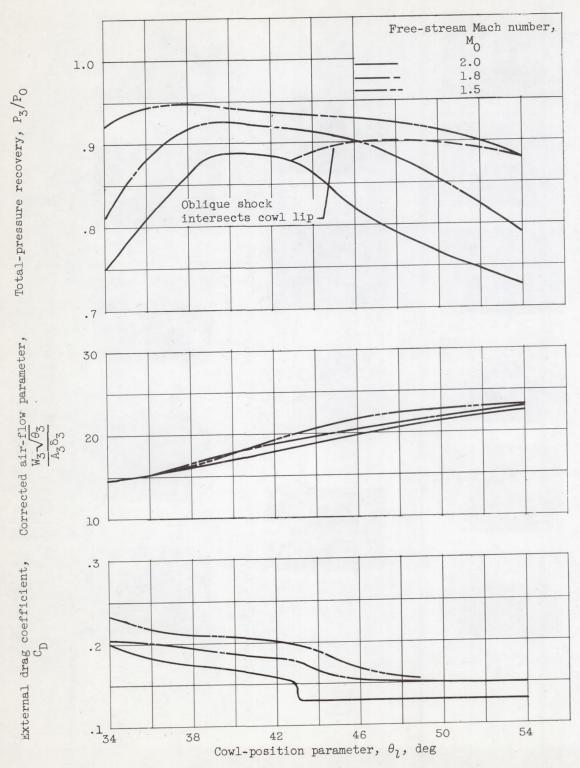


Figure 5. - Effect of spike translation on inlet characteristics at critical operation for zero angle of attack.

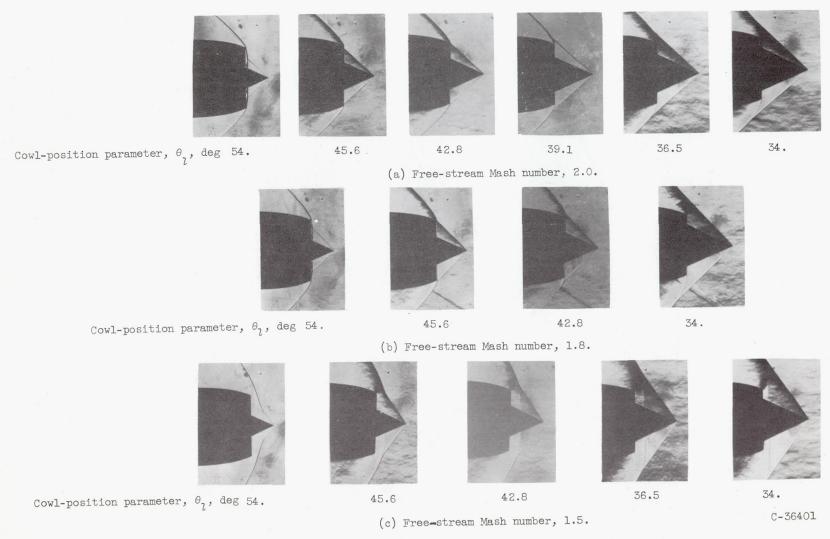


Figure 6. - Schlieren photographs of translating-spike inlet for various spike positions at critical operation and zero angle of attack.

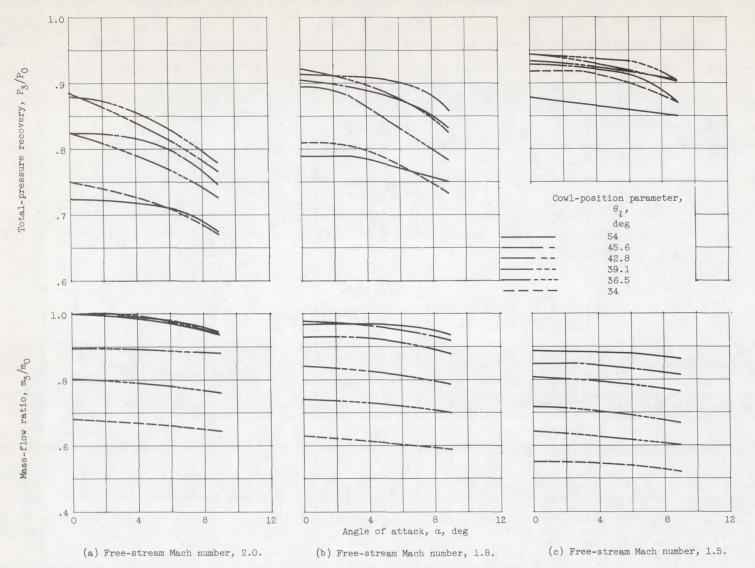


Figure 7. - Effect of angle of attack on translating-spike-inlet characteristics at critical operation.

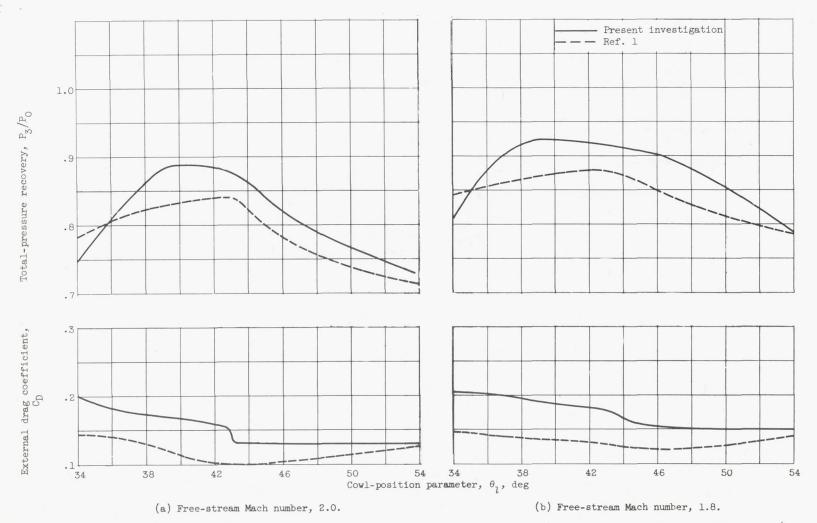


Figure 8. - Comparison of inlet characteristics at critical operation for two translating-spike-inlet designs.

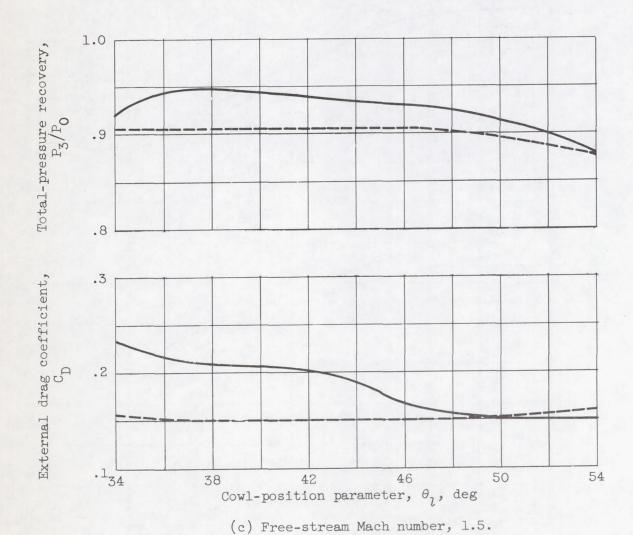


Figure 8. - Concluded. Comparison of inlet characteristics at critical operation for two translating-spike inlet designs.

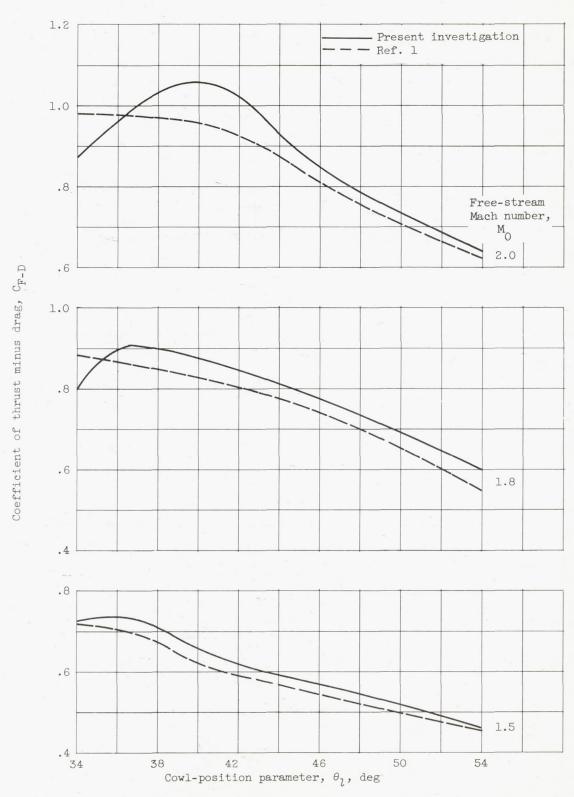


Figure 9. - Thrust-minus-drag comparison at critical operation for two translating-spike inlet designs.

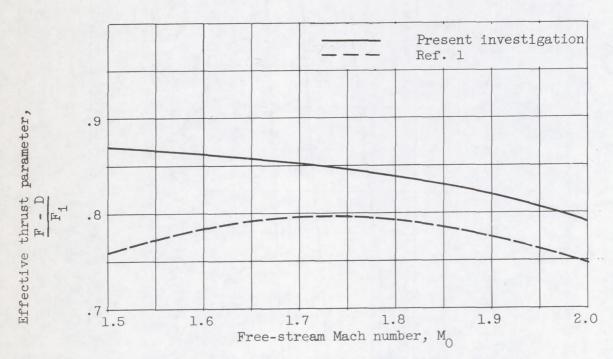


Figure 10. - Performance of turbojet engine matched with different translating-spike inlets. Inlet sized for zero mass-flow spillage at free-stream Mach number of 2.0 for altitude of 35,000 feet and above.

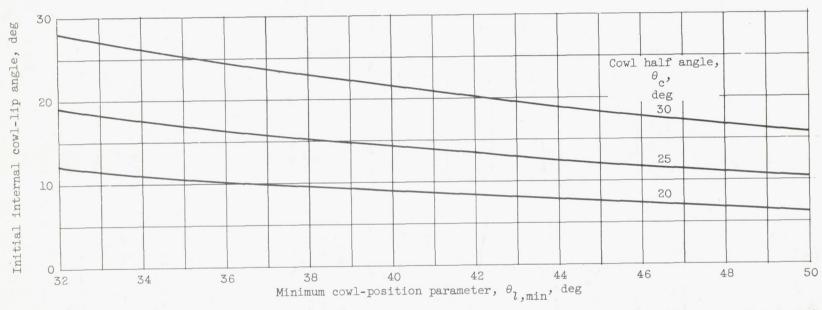


Figure 11. - Required initial internal cowl-lip angle for translating-spike inlet designed for no net internal contraction.